

Equivariant Conditional Neural Processes

Peter Holderrieth¹ Michael Hutchinson¹ Yee Whye Teh^{1,2}

Abstract

We introduce Equivariant Conditional Neural Processes (EquivCNPs), a new member of the Neural Process family that models vector-valued data in an equivariant manner with respect to isometries of \mathbb{R}^n . In addition, we look at multi-dimensional Gaussian Processes (GPs) under the perspective of equivariance and find the sufficient and necessary constraints to ensure a GP over \mathbb{R}^n is equivariant. We test EquivCNPs on the inference of vector fields using Gaussian process samples and real-world weather data. We observe that our model significantly improves the performance of previous models. By imposing equivariance as constraints, the parameter and data efficiency of these models are increased. Moreover, we find that EquivCNPs are more robust against overfitting to local conditions of the training data.

1. Introduction

In recent years, deep neural networks have enjoyed huge success leading to advances in areas such as speech (Hinton et al., 2012) and visual object recognition (Krizhevsky et al., 2012). In typical supervised learning setups, we assume that the training data has been drawn from a function $F : \mathcal{X} \rightarrow \mathcal{Y}$ and we use the data to try to produce the best possible approximation of F via our model. Deep neural networks are able to fit incredibly complex functions F but the training procedure requires large amounts of data about a single task. In particular, in settings where we have little data about an individual task, these methods tend to perform poorly.

There exists many scenarios however where we may have little data about an individual task, but may have many examples of similar tasks. In these scenarios we can leverage this data about related tasks to learn the commonalities between tasks and perform better on all tasks overall. One way to model this is to place a distribution over these task func-

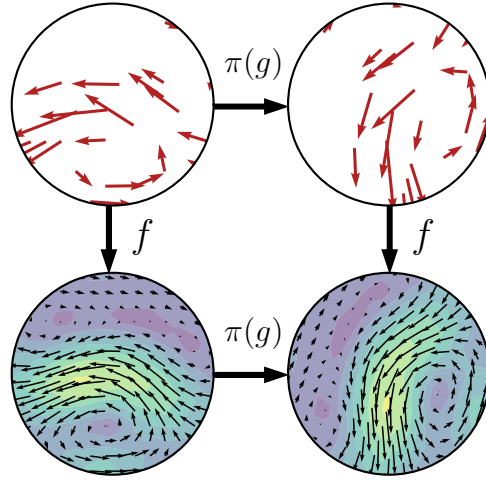


Figure 1. A demonstration of the meaning of equivariance for functions acting on vector fields. The function f embeds a set of points (red arrows) to a vector field embedding. It is equivariant to the action of π .

tions known as stochastic processes (SPs). The prototypical example of these are Gaussian Processes (GPs). Learning in GPs corresponds to Bayesian inference by conditioning on observed values. While exact inference is possible in these models, it quickly becomes intractable as the number of observations grows.

As an alternative, Garnelo et al. (2018a) introduced Conditional Neural Processes (CNPs). CNPs can be trained by usual gradient descent methods and produce probabilistic predictions about new locations conditioned on observed data much faster than for GPs.

Another recent trend to make deep learning models use data more efficiently is to implement prior beliefs about invariances and equivariances directly into the architecture of the model (Cohen & Welling, 2016a; Dieleman et al., 2016). Models fit to data that contain these symmetries have been shown to be significantly more data and parameter efficient than counterparts that do not have these symmetries built in (Weiler & Cesa, 2019). By implementing equivariance directly into the model architecture, we increase the parameter efficiency which allows us to build deeper architectures. This will lead to improved results as long as the gain in parameter efficiency outweighs the loss by imposing equiv-

¹University of Oxford, United Kingdom ²DeepMind, United Kingdom. Correspondence to: Peter Holderrieth < peter.holderrieth@new.ox.ac.uk >.

ariance constraints.

Translation equivariance has long been studied in Gaussian Processes via stationary kernels and recent work has shown how to build translation equivariance into a CNP model (Gordon et al., 2019). However, models which are equivariant with respect to more general types of symmetries such as rotations and reflections have mostly confined to supervised learning problems so far and have not been studied in stochastic process models. Given that CNPs are built to learn from few data, it is natural to expect that building more general equivariances into these models will lead to significant improvements, too.

To illustrate equivariance in a CNP framework, let us consider figure 1. The input to the model is a discrete set of vectors, the red arrows, and the model predicts a continuous vector field from this data. Now imagine that we rotate the data set by $\pi(g)$ and let the model predict again. Naturally, we would expect the model to give the same predictions as before but rotated in the same way as the data set. In other words, we expect the model to be equivariant. We will construct a model that has this behaviour by design which we call Equivariant Conditional Neural Processes (EquivCNP).

Our main contributions are as follows:

1. We formulate the problem of building a probabilistic meta-learning model which is equivariant to geometric transformations such as rotations and reflections. As a solution to this, we present Equivariant Conditional Neural Processes.
2. We find sufficient and necessary constraints for a vector-valued Gaussian Process over \mathbb{R}^n to be equivariant.
3. We test EquivCNP on vector field regression and inference on real-world weather data and show that it outperforms previous models in these experiments.

2. Related Work

This work can be considered as merging various recent developments of machine learning and we will briefly position our work in the different areas which our work is related to.

Learning stochastic processes and meta-learning. A classical model for learning the distribution over functions (a “task domain”) are Gaussian processes (GPs), which have been widely used in machine learning (Rasmussen & Williams, 2005). However, since they require the inversion of a matrix, GPs have a high computational cost and adoptions of the GP model such as sparse GPs (Snelson & Ghahramani, 2006; Titsias, 2009) are motivated by making GP inference scale better in the number of data points. Similiarly, advances in deep learning were combined to

construct more flexible GPs and to build more expressive kernels (Damianou & Lawrence, 2013; Wilson et al., 2015). In contrast to adopting GP inference models, Garnelo et al. (2018a) introduced Conditional Neural Processes as a one-shot learning model which is fully constructed out of neural networks. As opposed to optimization based meta-learning methods (Finn et al., 2017; Andrychowicz et al., 2016), CNPs can be seen as an architecture based meta-learning method while still sharing their motivation of learning a whole domain of tasks instead of only one task.

Closely related to CNPs are Neural Processes (NPs) (Garnelo et al., 2018b) which have similiar architectures but are latent variable models. Therefore, NPs give consistent samples of a distribution over functions and they are trained by amortized variational inference. Similiar latent variable models of stochastic processes are the Variational Implicit Process (Ma et al., 2019) or Consistent Generative Query Networks (Kumar et al., 2018), which were introduced as a consistent version of Generative Query Networks (Eslami et al., 2018), similiar to CNPs for NPs. Both CNPs and NPs have been shown to be flexible scaffold models to combine them with other machine learning concepts such as attention (Kim et al., 2019) or convolutional neural networks (Gordon et al., 2019). Similiarly, this work will present another member in the CNP family.

Equivariance and symmetries in machine learning.

Our goal is to build a CNP model which exploit the geometric structure of the data by design. A classical example for exploiting the geometric structure of the data are the widely-applied convolutional neural networks (CNNs) which implement translational equivariance (LeCun et al., 1990) and are widely used for images. Motivated by the success of CNNs, there has been a great interest to build neural networks which are also designed to be equivariant with respect to rotations or reflections. Approaches use a wide range of techniques such as convolutions on groups (Cohen et al., 2018b; Kondor & Trivedi, 2018; Cohen & Welling, 2016a; Hoogeboom et al., 2018; Worrall & Brostow, 2018), cyclic permutations (Dieleman et al., 2016), Lie groups (Finzi et al., 2020) or a phase change of complex-valued feature maps (Worrall et al., 2016). For us, the flexible approach of Steerable CNNs and its various generalizations (Cohen & Welling, 2016b; Weiler et al., 2018; Weiler & Cesa, 2019) gave the most simple and concise way to build an equivariant CNP model. These methods use general group representations to restrict the space of convolutional layers to those which are also equivariant with respect to rotations and reflections. Recently, a general theory of equivariant CNNs is provided (Cohen et al., 2018a) with the goal of unifying the different approaches in the literature via the concept of homogenous spaces.

Apart from geometric symmetries, also invariances with respect to permutations have been a widely considered topic

(Zaheer et al., 2017; Lee et al., 2018) and these ideas also influenced the construction of the encoder in the CNP. Since CNPs return an approximation of the posterior distribution, our work will also consider equivariance in a probabilistic sense which was recently studied generally by Bloem-Reddy & Teh (2019).

Equivariant one-shot learning and meta-learning. The problem of building an equivariant one-shot and meta-learning methods has not been studied for general rotations and reflections before. However, Gordon et al. (2019) consider the case of translational equivariance and provide a good framework for further generalization. Zhou et al. (2020) built a meta-learning framework which *learns* the symmetries of the data while our model focuses on *using* symmetries to improve meta-learning architectures knowing the symmetries apriori.

3. Transforming Feature Fields and Stochastic Processes

We aim to build to a model which learns functions F of the form $F : \mathbb{R}^n \rightarrow \mathbb{R}^d$. Using the language of (Weiler & Cesa, 2019), we will call F a *steerable feature map* since we interpret F geometrically as mapping coordinates $\mathbf{x} \in \mathbb{R}^n$ to some d -dimensional feature $F(\mathbf{x})$. Intuitively, we should be able to rotate such a feature map as we could do with an ordinary geographical map or an image. In this section, we make this rigorous using group and representation theory. See appendix A for a brief introduction to groups and representation theory.

In the following, let $E(n)$ be the group of isometries on \mathbb{R}^n . Let $T(n)$ be the group of all translations $t_{\mathbf{x}}$ of the form $t_{\mathbf{x}}(\mathbf{x}') = \mathbf{x}' + \mathbf{x}$ for all $\mathbf{x}, \mathbf{x}' \in \mathbb{R}^n$, and let $O(n)$ be the group of $n \times n$ orthogonal rotation matrices. For the rest of the paper we will be interested in subgroups $G \subset E(n)$ which are the *semidirect product* of the translation group and a subgroup H of $O(n)$, so every $g \in G$ is a unique combination of a translation $t_{\mathbf{x}}$ and an orthogonal map $h \in H$:

$$g = t_{\mathbf{x}}h \quad (1)$$

We will call H the *fiber group*. Theoretically, one would pick $H = SO(n)$ or $H = O(n)$ (equivalently $G = SE(n), E(n)$). However, using finite subgroups H can be more computationally efficient, and give better empirical results (Weiler & Cesa, 2019). In particular, in dimension $n = 2$ we use the Dihedral groups $D(m)$, comprised of the rotations by $\frac{2\pi}{m}$ and mirroring, and the Cyclic groups $C(m)$, comprised of rotations by $\frac{2\pi}{m}$.

We can use G to define the transformation of feature maps F . For this, we need a linear representation $\rho : H \rightarrow \text{GL}(\mathbb{R}^d)$ of the fiber group H . The action of G on a steerable feature

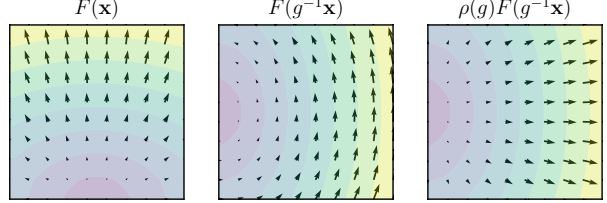


Figure 2. Demonstration of the transformation of tangent fields on \mathbb{R}^2 under the action of $SE(2)$. Color represents the norm of vector at each point.

map F is then defined as

$$g.F(\mathbf{x}) = \rho(h)F(g^{-1}\mathbf{x}) \quad (2)$$

where $g = t_{\mathbf{x}}h \in G$. In group theory, this is called the induced representation of H on G denoted by $\text{Ind}_H^G \rho$. In allusion to physics, one now uses the term *feature field* referring to the feature map $F : \mathbb{R}^n \rightarrow \mathbb{R}^d$ together with its corresponding law of transformation given by the fiber representation ρ . We write \mathcal{F}_ρ for the space of these fields. Typical examples include:

1. **Scalar fields** have feature maps $F : \mathbb{R}^n \rightarrow \mathbb{R}$ with scalar output and the trivial fiber representation:

$$g.F(\mathbf{x}) = F(g^{-1}\mathbf{x}) \quad (3)$$

Examples include greyscale images or temperature maps.

2. **Vector fields** have feature maps $F : \mathbb{R}^n \rightarrow \mathbb{R}^n$ where $F(\mathbf{x})$ describes a direction in \mathbb{R}^n and the fiber representation the identity ($\rho(h) = h$):

$$g.F(\mathbf{x}) = hF(g^{-1}\mathbf{x}) \quad (4)$$

Examples include electric fields or wind maps.

3. **Stacked fields**: given fields F_1, \dots, F_n with fiber representations ρ_1, \dots, ρ_n we can stack them to $F = (F_1, \dots, F_n)$ with fiber representation as the sum $\rho = \rho_1 \oplus \dots \oplus \rho_n$. Examples would include a combined wind and temperature map.

Figure 2 demonstrates for vector fields why the transformation defined here is a sensible notion to consider. We see that the action defined produces the intuitively correct behaviour. Since all fiber groups H of interest are compact, we can assume that ρ is an orthogonal representation, i.e. $\rho(h) \in O(d)$ for all $h \in H$.

In this work, we are interested in learning not only one feature field F but a probability distribution P over \mathcal{F}_ρ , i.e. a stochastic process over feature fields F . For example, P

could describe the distribution of all wind directions over a specific region. If $F \sim P$ is a random feature field and $g \in G$, we can define the transformed stochastic process $g.P$ as the distribution of $g.F$.

Finally, from a sample $F \sim P$, our model observes only a finite set of input-output pairs $Z = \{(\mathbf{x}_i, \mathbf{y}_i)\}_{i=1}^n$ where \mathbf{y}_i equals $F(\mathbf{x}_i)$ plus potentially some noise. The induced representation naturally translates to a transformation of Z under G via

$$g.Z := \{(g\mathbf{x}_i, \rho(h)\mathbf{y}_i)\}_{i=1}^n \quad (5)$$

4. Equivariant Stochastic Process Models

In a Bayesian approach, we can consider P as a prior and given an observed data set Z we can consider the posterior, i.e. the conditional distribution P_Z of F given Z . We call a posterior map $Z \mapsto P_Z$ equivariant, if

$$P_{g.Z} = g.P_Z \quad (6)$$

In many cases, we believe our data generating distribution P to be invariant with respect to transformations in G . In this case, it is natural to consider a G -invariant prior over \mathcal{F}_ρ . The following proposition states that if we have such a prior, then the posterior of our model will be equivariant.

Proposition 1. *Let P be a stochastic process over \mathcal{F}_ρ . Then the true posterior map $Z \mapsto P_Z$ is G -equivariant if and only if P is G -invariant, i.e. if and only if*

$$P = g.P \quad \text{for all } g \in G \quad (7)$$

The proof of this can be found in appendix B.1.

In most real-world scenarios, it may not be possible to exactly compute the posterior and our goal is to build a model Q which returns an approximation Q_Z of P_Z . Given proposition 1, it is then natural to construct an approximate inference model Q which is itself equivariant as this reflects the nature of the true posterior.

We will see applications of these ideas to GPs and CNPs in sections 5 and 6.

5. Equivariant Gaussian Processes

A widely-studied example of stochastic processes are Gaussian Processes (GPs). Here we will look at Gaussian processes under the lens of equivariance. Since we are interested in vector-valued functions $F : \mathbb{R}^n \rightarrow \mathbb{R}^d$, will be interested in matrix-valued positive definite kernels $K : \mathbb{R}^n \times \mathbb{R}^n \rightarrow \mathbb{R}^{d \times d}$ (Álvarez et al., 2012).

In the case of GPs, we assume that for every $\mathbf{x}, \mathbf{x}' \in \mathbb{R}^n$, it holds that $F(\mathbf{x})$ is normally distributed with mean $\mathbf{m}(\mathbf{x})$

and covariances $\text{Cov}(F(\mathbf{x}), F(\mathbf{x}')) = K(\mathbf{x}, \mathbf{x}')$. We write $\mathcal{GP}(\mathbf{m}, K)$ for the stochastic process defined by this.

We can fully characterize all mean functions and kernels leading to equivariant GPs:

Theorem 1. *Let $G = T(n) \rtimes H$ and $\rho : H \rightarrow O(\mathbb{R}^d)$ be a fiber representation. A Gaussian process $\mathcal{GP}(\mathbf{m}, K)$ is G -equivariant for any noise parameter $\sigma^2 > 0$ if and only if it holds that*

$$\begin{aligned} 1. \quad & \mathbf{m}(\mathbf{x}) = \mathbf{m} \in \mathbb{R}^d \text{ is constant such that for all } h \in H \\ & \rho(h)\mathbf{m} = \mathbf{m} \end{aligned} \quad (8)$$

2. *K is fulfils the following two conditions:*

$$(a) \quad K \text{ is stationary, i.e. for all } \mathbf{x}, \mathbf{x}' \in \mathbb{R}^n$$

$$K(\mathbf{x}, \mathbf{x}') = K(\mathbf{x} - \mathbf{x}', \mathbf{0}) = \hat{K}(\mathbf{x} - \mathbf{x}') \quad (9)$$

$$(b) \quad K \text{ satisfies the angular constraint, i.e. for all } \mathbf{x}, \mathbf{x}' \in \mathbb{R}^n, h \in H \text{ it holds that}$$

$$K(h\mathbf{x}, h\mathbf{x}') = \rho(h)K(\mathbf{x}, \mathbf{x}')\rho(h)^T \iff (10)$$

$$\hat{K}(h\mathbf{x}) = \rho(h)\hat{K}(\mathbf{x})\rho(h)^T \quad (11)$$

If this is the case, we call K ρ -equivariant from now on.

The proof of this can be found in appendix B.2.

A popular example to model vector-valued functions is to simply to use d independent GPs with a stationary scalar kernel $k : \mathbb{R}^n \rightarrow \mathbb{R}$. This leads to a kernel $K(\mathbf{x}) = k(\mathbf{x})I$ and can be easily seen to be equivariant.

As a non-trivial example of equivariant kernels, we will also consider the divergence-free and curl-free kernels used in physics introduced by Macêdo & Castro (2010) which allow us to model divergence-free and curl-free fields such as electric or magnetic fields (see appendix C).

6. Equivariant Conditional Neural Processes

Conditional Neural Processes were introduced as an alternative model to Gaussian processes. While GPs require to explicitly model the prior P and can perform exact posterior inference, CNPs aim to learn an approximation to the posterior map ($Z \mapsto P_Z$) directly, only implicitly learning a prior from data. Generally speaking, the underlying architecture is a model which returns a mean function $\mathbf{m}_Z : \mathbb{R}^n \rightarrow \mathbb{R}^d$ and a covariance function $\Sigma_Z : \mathbb{R}^n \rightarrow \mathbb{R}^{d \times d}$ from a context set Z . It makes the simplifying assumption that given Z the functions values $F(\mathbf{x})$ are independent and normally distributed

$$F(\mathbf{x}) \sim \mathcal{N}(\mathbf{m}_Z(\mathbf{x}), \Sigma_Z(\mathbf{x})), \quad F(\mathbf{x}) \perp F(\mathbf{x}') \quad (12)$$

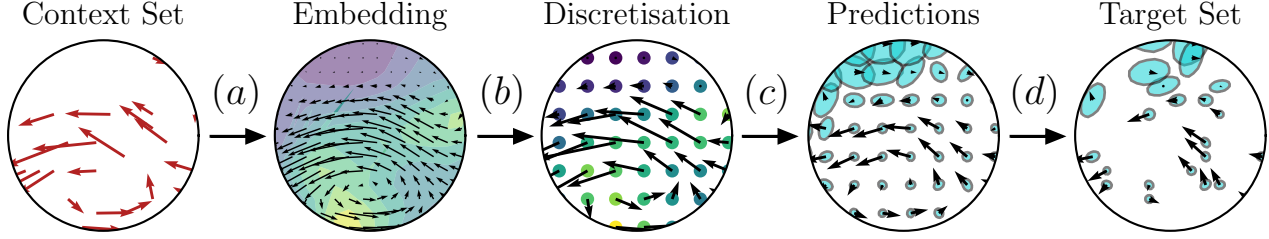


Figure 3. Equiv CNP model illustration. (a) Embed the context set into a function (b) Discretise this embedding on a regular grid. (c) Predict the mean and covariance of the conditional stochastic process on the grid of points. (d) Use kernel smoothing to predict the mean and covariance at target locations.

Let us call a model as in eq. (12) a *conditional process model*. For such models, we can easily characterize equivariance. To do this, we introduce here the concept of the *covariance representation* of ρ . We define this to be the representation $\rho_\Sigma : H \rightarrow S(d)$ on the space of symmetric $d \times d$ -matrices $S(d)$ defined by

$$\rho_\Sigma(h)A = \rho(h)A\rho(h)^T \quad (13)$$

We specify a law of transformation by considering \mathbf{m}_Z as the *mean feature field* in \mathcal{F}_ρ and Σ_Z as the *covariance feature field* in $\mathcal{F}_{\rho_\Sigma}$. This is natural as the following proposition shows:

Proposition 2. *A conditional process model is G -equivariant if and only if the mean and covariance feature maps are G -equivariant, i.e. if it holds*

$$\mathbf{m}_{g,Z} = g.\mathbf{m}_Z \quad (14)$$

$$\Sigma_{g,Z} = g.\Sigma_Z \quad (15)$$

for all $g \in G$ and context sets Z .

The proof is straight-forward and can be found in appendix B.3.

In the following, we will restrict ourselves to perform inference from data sets of multiplicity 1, i.e. data sets $Z = \{(\mathbf{x}_i, \mathbf{y}_i)\}_{i=1}^m$ where $\mathbf{x}_i \neq \mathbf{x}_j$ for all $i \neq j$. We denote the collection of all such data sets with \mathcal{Z}_ρ^1 meaning that they transform under ρ (see eq. (5)).

Moreover, we assume that there is no order in a data set Z , i.e. we aim to build models which are not only G -equivariant but also invariant to permutations of Z .

We can characterize all such conditional process models by picking $\rho_{\text{in}} = \rho$ and $\rho_{\text{out}} = \rho \oplus \rho_\Sigma$ in the following generalization of the ConvDeepSets theorem of Gordon et al. (2019):

Theorem 2 (EquivDeepSets). *A function $\Phi : \mathcal{Z}_{\rho_{\text{in}}}^1 \rightarrow \mathcal{F}_{\rho_{\text{out}}}$ is G -equivariant and permutation invariant if and only if it has a representation of the form*

$$\Phi(Z) = \Psi(E(Z))$$

for all $Z = \{(\mathbf{x}_i, \mathbf{y}_i)\}_{i=1}^m \in \mathcal{Z}_{\rho_{\text{in}}}^1$ where

1. $E(Z) = \sum_{i=1}^m K(\cdot, \mathbf{x}_i)\phi(\mathbf{y}_i)$
2. $\phi(\mathbf{y}) = (1, \mathbf{y})^T \in \mathbb{R}^{d+1}$.
3. $K : \mathbb{R}^n \times \mathbb{R}^n \rightarrow \mathbb{R}^{(d+1) \times (d+1)}$ is an ρ_E -equivariant strictly positive definite kernel (see theorem 1).
4. $\Psi : \mathcal{F}_{\rho_E} \rightarrow \mathcal{F}_{\rho_{\text{out}}}$ is a G -equivariant functions.

where we coin $\rho_E = \mathbf{1} \oplus \rho_{\text{in}}$ the embedding representation.

Additionally, by imposing extra constraints (see appendix B.4), we can also ensure that Φ is continuous.

The proof of this can be found in appendix B.4. Using this, we can start to build EquivCNPs by building an encoder E and a decoder Ψ as specified in the theorem.

The form of the encoder only depends on the choice of a kernel K which is equivariant under ρ_E . An easy but effective way of doing this is to pick a kernel K_0 which is equivariant under ρ (see section 5) and a scalar kernel $k : \mathbb{R}^n \rightarrow \mathbb{R}$ and then use the block-version $K = k \oplus K_0$.

6.1. Decoder

By theorem 2, it remains to construct a flexible and learnable G -equivariant decoder Ψ . In practice, this will only be possible to compute in a discretized way and so it will be only approximately equivariant.

To construct such maps, we will use steerable CNNs (Cohen & Welling, 2016b; Weiler & Cesa, 2019; Weiler et al., 2018). In theory, a layer of such a network is an equivariant function $\Psi : \mathcal{F}_{\rho_{\text{in}}} \rightarrow \mathcal{F}_{\rho_{\text{out}}}$ where we are free to choose fiber representations $\rho_{\text{in}}, \rho_{\text{out}}$.

Steerable convolutional layers are defined by a constrained kernel $\kappa : \mathbb{R}^n \rightarrow \mathbb{R}^{c_{\text{out}} \times c_{\text{in}}}$ such that the map

$$[\kappa * F](\mathbf{x}) = \int \kappa(\mathbf{x}, \mathbf{x}') F(\mathbf{x}') d\mathbf{x} \quad (16)$$

is G -equivariant. These layers serve as the learnable, parameterizable functions. Equivariant activation functions are

applied pointwise to F between convolution layers to create a CNN. These are activation functions $\sigma : \mathbb{R}^{c_{\text{in}}} \rightarrow \mathbb{R}^{c_{\text{out}}}$ such that

$$\sigma(\rho_{\text{in}}(h)\mathbf{x}) = \rho_{\text{out}}(h)\sigma(\mathbf{x}) \quad (17)$$

As a decoder of our model, we use a stack of equivariant convolutional layers intertwined with equivariant activation functions. The convolutions in eq. (16) are computed in a discretized manner after sampling $E(Z)$ on a grid $\mathcal{G} \subset \mathbb{R}^n$. We use ρ_E as input fiber representation of the first layer, while we are free to choose the representations of any intermediate layer. Therefore, the output of the neural network will be a discretized version of a function and we use kernel smoothing to extend the output of the network to the whole space.

6.2. Covariance Activation Functions

The output of an equivariant neural network has outputs in \mathbb{R}^c for some c . Therefore, we need an additional component to equivariantly map $\mathbb{R}^c \rightarrow \mathbb{R}^{d \times d}$ such that the output is a positive definite covariance matrix.

We introduce the following concept:

Definition 1. Let $\rho : H \rightarrow GL(\mathbb{R}^d)$ be a fiber representation. An **equivariant covariance activation function** is a map $\eta : \mathbb{R}^c \rightarrow \mathbb{R}^{d \times d}$ for some $c \in \mathbb{N}$ which fulfills

1. For every $\mathbf{y} \in \mathbb{R}^c$ it holds that $\eta(\mathbf{y})$ is a symmetric, positive semi-definite matrix.
2. There is an input representation $\rho_\eta : H \rightarrow GL(\mathbb{R}^c)$ such that η is G -equivariant

$$\eta(\rho_\eta(h)\mathbf{y}) = \rho_\Sigma(h)\eta(\mathbf{y}) \quad (18)$$

In our case, we used a *quadratic covariance activation function* which we define by

$$\eta : \mathbb{R}^{d \times d} \rightarrow \mathbb{R}^{d \times d}, \quad \eta(A) = AA^T$$

Considering $A = (a_1, \dots, a_D) \in \mathbb{R}^{d^2}$ as a vector by stacking the columns, the input representation is then $\rho_\eta = \rho \oplus \dots \oplus \rho$ as the d -times sum of ρ . With this, it is straight forward to see that η is equivariant.

6.3. Full model

With this, we can finally summarize the architecture of the EquivCNP (see fig. 4 for a block diagram and fig. 3 for a depiction of data flowing through the model):

1. The **encoder** produces an embedding of a data set Z as a function $E(Z)$.

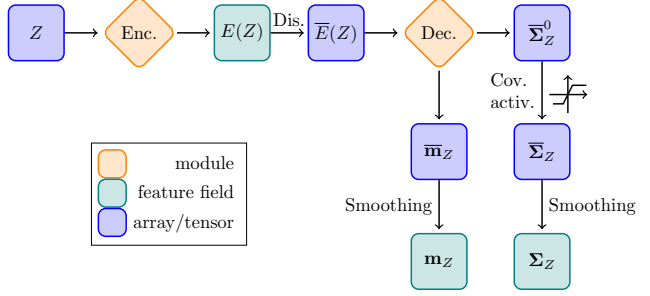


Figure 4. EquivCNP model architecture

2. A discretization $\bar{E}(Z)$ serves as input for the **decoder**, a stack of equivariant convolutional layers and equivariant activation functions with input fiber representation ρ_E and output fiber representation $\rho \oplus \rho_\eta$.
3. The output of the decoder is split in a mean part and a covariance part. On the covariance part, we apply the covariance activation function η to obtain covariance matrices.
4. The grid values of the mean and the covariances are extended to the whole space \mathbb{R}^n via kernel smoothing by a scalar kernel.

We train the model similar to the CNP by iteratively sampling a data set Z and splitting it randomly in a context set Z_C and a target set Z_T . The context set Z_C is then passed forward through the EquivCNP model and the mean log-likelihood of the target $Z_T = \{(\mathbf{x}'_i, \mathbf{y}'_i)\}_{i=1}^m$ is computed. In brief, we minimize the loss

$$-\mathbb{E}_{Z_C, Z_T \sim P} \left[\frac{1}{m} \sum_{i=1}^m \log \mathcal{N}(\mathbf{y}'_i; \mathbf{m}_{Z_C}(\mathbf{x}'_i), \Sigma_{Z_C}(\mathbf{x}'_i)) \right]$$

by gradient descent methods.

In sum, this gives a CNP model, which up to discretization errors is equivariant with respect to arbitrary transformations from the group G and invariant to permutations.

7. Experiments

Finally, we provide empirical evidence that equivariance is a helpful bias in stochastic process models by showing that EquivCNPs outperform previous models. We use synthetic data sampled from equivariant Gaussian process vector fields and real-world weather data. For the implementation of equivariant convolutional layers, we use the library recently introduced by [Weiler & Cesa \(2019\)](#) and we apply the Adam optimizer ([Kingma & Ba, 2015](#)) to train the model. For details on the architectures and training procedure, see appendix D.

7.1. GP Vector Fields

A common baseline task for CNPs is regression on samples from a Gaussian process $\mathcal{GP}(0, K)$ (Garnelo et al., 2018a; Gordon et al., 2019). The advantage of using synthetic GP data instead of real data is that in this case we can compare the output of our model directly with the true posterior. Here, we consider the task of learning 2D vector fields $F : \mathbb{R}^2 \rightarrow \mathbb{R}^2$ which are samples of a GP $\mathcal{GP}(0, K)$ with 3 different kernels: diagonal RBF-kernel, divergence-free kernel and curl-free kernel (see appendix C).

We run extensive experiments comparing the EquivCNP with the CNP and the translation-equivariant counterpart Convolutional CNPs (ConvCNPs) (Gordon et al., 2019). For the EquivCNP, we have chosen the fiber groups $H = C_4, D_4, D_8, C_{16}$. Each fiber group imposes a different level of rotation and reflection equivariance on the model and our goal is to evaluate to which extent equivariance in the model improves the results.

For every model, we optimized the model architecture independently starting with a number of layers ranging from 3 to 9 and with a number of parameters from 20000 to 2 million. As a measure of performance, we use the mean log-likelihood. The maximum is obtained by Monte Carlo sampling using the true GP posterior.

In table 1, the results are presented. Overall, one can see that the EquivCNP clearly outperforms previous models by reducing the difference to the GP baseline by more than a half.

In addition, we observe that fiber larger groups lead to slightly worse results. Although theoretically they should outperform models with smaller fiber groups, we propose that practical limitations such as optimization and discretization of the model favors smaller fiber groups since they still allow for some asymmetries in the data and to compensate for numerical errors.

7.2. ERA5 Weather Data

To evaluate the performance of the EquivCNP model on a real-world data set, we retrieved weather data from the global ERA5 data set.¹ We extracted the data for a cyclic region surrounding Memphis, Tennessee, and from a region of the same size in Hubei province, Southern China (see appendix D for details).

Every sample F corresponds to one weather map of temperature, pressure and wind in the region at one single point in time. We give the models the task to infer a wind vector field from a data Z of pairs (\mathbf{x}, \mathbf{y}) where $\mathbf{y} = (y^t, y^p, y_1^w, y_2^w) \in \mathbb{R}^4$ gives the temperature, pressure and wind at point \mathbf{x} . In particular, the output features are only a subset of the input features. To deal with such

¹We obtained this data using Copernicus Climate Change Service Information [2020].

a task, we can simply pick different input and output fiber representations for the EquivCNP

$$\rho_{\text{in}} = \mathbf{1} \oplus \mathbf{1} \oplus \rho_{\text{Id}}, \quad \rho_{\text{out}} = \rho_{\text{Id}}$$

where we pick the trivial representation $\mathbf{1}$ for the scalar values temperature and pressure and the identity representation ρ_{Id} for the wind vector field.

As a first experiment, we split the US data set in a train, validation and test data set and train and test the models accordingly. We observe that the EquivCNP outperforms previous models like the CNP and the ConvCNP with a significant margin for all considered fiber groups (see table 2). In addition, we observe again that a relatively small fiber group C_4 leads to the best results. Inference from weather data is clearly not exactly equivariant due to local differences such as altitude and distance to the sea. Therefore, it seems that an EquivCNP model with small fiber groups like C_4 enables us to exploit the equivariant patterns much better than the ConvCNP and CNP but leave enough flexibility to account for asymmetric patterns.

As a second experiment, we train the models on the US data but test the performance on the China data this time. By doing this, we can evaluate to which extent the models have learnt the inherent dynamics of the weather instead of adopting only to local conditions. Again, the EquivCNP clearly outperforms other models. Intuitively, posing a higher equivariance restriction on the model makes it less adapting to special local circumstances and makes it more robust when changing its environment. That is why we observe that the CNP, the ConvCNP and our model with fiber group C_4 has a significant loss in performance than EquivCNP models with bigger fiber groups such as C_{16}, D_8, D_4 . In applications like robotics where environments constantly change this robustness of the EquivCNP might be advantageous.

8. Conclusion

In this work, we have introduced Equivariant Conditional Neural Processes, a model that combines recent developments in the design of equivariant neural networks with the family of Conditional Neural Processes. We showed that it improves the results of previous models and is more robust to changes in the underlying distribution. We have also theoretically motivated the design of equivariant stochastic process models by showing that invariance in the data distribution naturally leads to equivariance and we fully characterized equivariant Gaussian processes for steerable functions over \mathbb{R}^n .

So far, our model cannot capture dependencies between the marginals of the posterior and further work could study how to overcome this limitation. Recent developments in the design of neural networks explore more general geometric spaces and encourage more exploration in this direction. To sum up, this work shows that building equivariance into

Model	RBF	Curl-free	Div-free
CNP	-4.24 \pm 0.00	-0.750 \pm 0.004	-0.752 \pm 0.006
ConvCNP	-3.88 \pm 0.01	-0.541 \pm 0.004	-0.533 \pm 0.001
EquivCNP (C_{16})	-3.71 \pm 0.02	-0.476 \pm 0.005	-0.480 \pm 0.008
EquivCNP (D_4)	-3.72 \pm 0.03	-0.471 \pm 0.002	-0.477 \pm 0.005
EquivCNP (D_8)	-3.68 \pm 0.03	-0.462 \pm 0.005	-0.467 \pm 0.008
EquivCNP (C_4)	-3.66 \pm 0.00	-0.461 \pm 0.003	-0.464 \pm 0.007
GP	-3.50	-0.410	-0.411

Table 1. Log-likelihoods on GP vector field (mean and standard deviation over 5 runs).

a meta-learning or stochastic process model is a fruitful ground for future work. We believe this could be a substantial step of building machine learning models which are more data-efficient and more adaptable to new learning tasks.

References

Álvarez, M. A., Rosasco, L., and Lawrence, N. D. Kernels for vector-valued functions: A review. *Found. Trends Mach. Learn.*, 4(3):195–266, March 2012. ISSN 1935-8237. doi: 10.1561/2200000036. URL <https://doi.org/10.1561/2200000036>.

Andrychowicz, M., Denil, M., Colmenarejo, S. G., Hoffman, M. W., Pfau, D., Schaul, T., and de Freitas, N. Learning to learn by gradient descent by gradient descent. *CoRR*, abs/1606.04474, 2016. URL <http://arxiv.org/abs/1606.04474>.

Artin, M. *Algebra*. Pearson Prentice Hall, 2011. ISBN 9780132413770. URL <https://books.google.co.uk/books?id=S6GSAgAAQBAJ>.

Bloem-Reddy, B. and Teh, Y. W. Probabilistic symmetry and invariant neural networks. *arXiv preprint arXiv:1901.06082*, 2019.

Bröcker, T. and Dieck, T. *Representations of Compact Lie Groups*. Graduate Texts in Mathematics. Springer Berlin Heidelberg, 2003. ISBN 9783540136781. URL <https://books.google.co.uk/books?id=AfBzWL5bIIQ>.

Cohen, T., Geiger, M., and Weiler, M. A general theory of equivariant CNNs on homogeneous spaces. *CoRR*, abs/1811.02017, 2018a. URL <http://arxiv.org/abs/1811.02017>.

Cohen, T. S. and Welling, M. Group equivariant convolutional networks. *CoRR*, abs/1602.07576, 2016a. URL <http://arxiv.org/abs/1602.07576>.

Cohen, T. S. and Welling, M. Steerable CNNs. *CoRR*, abs/1612.08498, 2016b. URL <http://arxiv.org/abs/1612.08498>.

Cohen, T. S., Geiger, M., Köhler, J., and Welling, M. Spherical CNNs. *CoRR*, abs/1801.10130, 2018b. URL <http://arxiv.org/abs/1801.10130>.

Damianou, A. and Lawrence, N. Deep Gaussian processes. volume 31 of *Proceedings of Machine Learning Research*, pp. 207–215, Scottsdale, Arizona, USA, 29 Apr–01 May 2013. PMLR. URL <http://proceedings.mlr.press/v31/damianou13a.html>.

Dieleman, S., Fauw, J. D., and Kavukcuoglu, K. Exploiting cyclic symmetry in convolutional neural networks. *CoRR*, abs/1602.02660, 2016. URL <http://arxiv.org/abs/1602.02660>.

Eslami, S. M. A., Jimenez Rezende, D., Besse, F., Viola, F., Morcos, A. S., Garnelo, M., Ruderman, A., Rusu, A. A., Danihelka, I., Gregor, K., Reichert, D. P., Buesing, L., Weber, T., Vinyals, O., Rosenbaum, D., Rabinowitz, N., King, H., Hillier, C., Botvinick, M., Wierstra, D., Kavukcuoglu, K., and Hassabis, D. Neural scene representation and rendering. *Science*, 360(6394):1204–1210, 2018. ISSN 0036-8075. doi: 10.1126/science.aar6170. URL <https://science.sciencemag.org/content/360/6394/1204>.

Finn, C., Abbeel, P., and Levine, S. Model-agnostic meta-learning for fast adaptation of deep networks. *CoRR*, abs/1703.03400, 2017. URL <http://arxiv.org/abs/1703.03400>.

Finzi, M., Stanton, S. C., Izmailov, P., and Wilson, A. Generalizing convolutional neural networks for equivariance to lie groups on arbitrary continuous data. *arXiv*, abs/2002.12880, 2020.

Garnelo, M., Rosenbaum, D., Maddison, C., Ramalho, T., Saxton, D., Shanahan, M., Teh, Y. W., Rezende, D., and Eslami, S. M. A. Conditional neural processes. In Dy,

Model	US	China
CNP	0.036 \pm 0.017	-2.456 \pm 0.365
ConvCNP	0.898 \pm 0.045	-0.890 \pm 0.059
EquivCNP (C_{16})	1.094 \pm 0.015	-0.550 \pm 0.073
EquivCNP (D_8)	1.032 \pm 0.011	-0.539 \pm 0.129
EquivCNP (D_4)	1.037 \pm 0.037	-0.429 \pm 0.067
EquivCNP (C_4)	1.255 \pm 0.019	-0.578 \pm 0.173

Table 2. Log-likelihoods on ERA5 weather data (mean and standard deviation over 5 runs).

J. and Krause, A. (eds.), *Proceedings of the 35th International Conference on Machine Learning*, volume 80 of *Proceedings of Machine Learning Research*, pp. 1704–1713, Stockholm, Sweden, 10–15 Jul 2018a. PMLR. URL <http://proceedings.mlr.press/v80/garnelo18a.html>.

Garnelo, M., Schwarz, J., Rosenbaum, D., Viola, F., Rezende, D. J., Eslami, S. M. A., and Teh, Y. W. Neural processes. *CoRR*, abs/1807.01622, 2018b. URL <http://arxiv.org/abs/1807.01622>.

Gordon, J., Bruinsma, W. P., Foong, A. Y., Requeima, J., Dubois, Y., and Turner, R. E. Convolutional conditional neural processes. *arXiv preprint arXiv:1910.13556*, 2019.

Hinton, G., Deng, L., Yu, D., Dahl, G. E., Mohamed, A., Jaitly, N., Senior, A., Vanhoucke, V., Nguyen, P., Sainath, T. N., and Kingsbury, B. Deep neural networks for acoustic modeling in speech recognition: The shared views of four research groups. *IEEE Signal Processing Magazine*, 29(6):82–97, 2012.

Hoogeboom, E., Peters, J. W. T., Cohen, T. S., and Welling, M. Hexaconv. *CoRR*, abs/1803.02108, 2018. URL <http://arxiv.org/abs/1803.02108>.

Kim, H., Mnih, A., Schwarz, J., Garnelo, M., Eslami, S. M. A., Rosenbaum, D., Vinyals, O., and Teh, Y. W. Attentive neural processes. *CoRR*, abs/1901.05761, 2019. URL <http://arxiv.org/abs/1901.05761>.

Kingma, P. and Ba, J. Adam: A method for stochastic optimization, arxiv (2014). *arXiv preprint arXiv:1412.6980*, 106, 2015.

Kondor, R. and Trivedi, S. On the generalization of equivariance and convolution in neural networks to the action of compact groups. *CoRR*, abs/1802.03690, 2018. URL <http://arxiv.org/abs/1802.03690>.

Krizhevsky, A., Sutskever, I., and Hinton, G. Imagenet classification with deep convolutional neural networks. *Neural Information Processing Systems*, 25, 01 2012. doi: 10.1145/3065386.

Kumar, A., Eslami, S. M. A., Rezende, D. J., Garnelo, M., Viola, F., Lockhart, E., and Shanahan, M. Consistent generative query networks. *CoRR*, abs/1807.02033, 2018. URL <http://arxiv.org/abs/1807.02033>.

LeCun, Y., Boser, B. E., Denker, J. S., Henderson, D., Howard, R. E., Hubbard, W. E., and Jackel, L. D. Handwritten digit recognition with a back-propagation network. In Touretzky, D. S. (ed.), *Advances in Neural Information Processing Systems 2*, pp. 396–404. Morgan-Kaufmann, 1990.

Lee, J., Lee, Y., Kim, J., Kosiorek, A. R., Choi, S., and Teh, Y. W. Set transformer. *CoRR*, abs/1810.00825, 2018. URL <http://arxiv.org/abs/1810.00825>.

Ma, C., Li, Y., and Hernández-Lobato, J. M. Variational implicit processes. In *International Conference on Machine Learning*, pp. 4222–4233, 2019.

Macêdo, I. and Castro, R. *Learning divergence-free and curl-free vector fields with matrix-valued kernels*. IMPA, 2010.

Paszke, A., Gross, S., Chintala, S., Chanan, G., Yang, E., DeVito, Z., Lin, Z., Desmaison, A., Antiga, L., and Lerer, A. Automatic differentiation in pytorch. 2017.

Rasmussen, C. E. and Williams, C. K. I. *Gaussian Processes for Machine Learning (Adaptive Computation and Machine Learning)*. The MIT Press, 2005. ISBN 026218253X.

Snelson, E. and Ghahramani, Z. Sparse Gaussian processes using pseudo-inputs. In Weiss, Y., Schölkopf, B., and Platt, J. C. (eds.), *Advances in Neural Information Processing Systems 18*, pp. 1257–1264. MIT Press, 2006.

Titsias, M. Variational learning of inducing variables in sparse Gaussian processes. volume 5 of *Proceedings of Machine Learning Research*, pp. 567–574, Hilton Clearwater Beach Resort, Clearwater Beach, Florida USA, 16–18 Apr 2009. PMLR. URL <http://proceedings.mlr.press/v5/titsias09a.html>.

Weiler, M. and Cesa, G. General $E(2)$ -equivariant steerable CNNs. In *Advances in Neural Information Processing Systems*, pp. 14334–14345, 2019.

Weiler, M., Geiger, M., Welling, M., and Cohen, W. B. 3d steerable CNNs: Learning rotationally equivariant features in volumetric data. *CoRR*, abs/1807.02547, 2018. URL <http://arxiv.org/abs/1807.02547>.

Wilson, A. G., Hu, Z., Salakhutdinov, R., and Xing, E. P. Deep kernel learning. *CoRR*, abs/1511.02222, 2015. URL <http://arxiv.org/abs/1511.02222>.

Worrall, D. E. and Brostow, G. J. Cubenet: Equivariance to 3d rotation and translation. *CoRR*, abs/1804.04458, 2018. URL <http://arxiv.org/abs/1804.04458>.

Worrall, D. E., Garbin, S. J., Turmukhambetov, D., and Brostow, G. J. Harmonic networks: Deep translation and rotation equivariance. *CoRR*, abs/1612.04642, 2016. URL <http://arxiv.org/abs/1612.04642>.

Zaheer, M., Kottur, S., Ravanbakhsh, S., Póczos, B., Salakhutdinov, R., and Smola, A. J. Deep sets. In

Proceedings of the 31st International Conference on Neural Information Processing Systems, NIPS'17, pp. 3394–3404, Red Hook, NY, USA, 2017. Curran Associates Inc. ISBN 9781510860964.

Zhou, A., Knowles, T., and Finn, C. Meta-learning symmetries by reparameterization. *arXiv preprint arXiv:2007.02933*, 2020.

Øksendal, B. *Stochastic Differential Equations: An Introduction with Applications*, volume 82. 01 2000. doi: 10.1007/978-3-662-03185-8.

A. Basics for Group and Representation Theory

A.1. Groups

This section gives basic definitions of groups and representations necessary to understand this work. We refer to the literature for a more detailed introduction (Artin, 2011; Bröcker & Dieck, 2003).

A **group** (G, \cdot) is a set G together with a function $\cdot : G \times G \rightarrow G, (g, h) \mapsto g \cdot h$ called **group operation** satisfying

1. (Associativity): $g \cdot (h \cdot i) = (g \cdot h) \cdot i$ for all $g, h, i \in G$
2. (Existence of a neutral element): There is a $e \in G$ such that: $e \cdot g = g \cdot e = g$ for all $g \in G$
3. (Existence of an inverse): For all $g \in G$, there is a g^{-1} such that $e = g^{-1} \cdot g = g \cdot g^{-1}$

If in addition, G satisfies

4. (Commutativity): $g \cdot h = h \cdot g$ for all $g, h \in G$

G is called **Abelian**.

If $\rho : G \rightarrow G'$ is a map between two groups, it is called a **group homomorphism** if $\rho(g \cdot g') = \rho(g) \cdot \rho(g')$. That is, the map preserves the action of the group. A **group isomorphism** is a homomorphism that is bijective. In the later case, G and G' are called isomorphic and we write $G \cong G'$. We simply write $g_1 g_2$ for $g_1 \cdot g_2$ if it is clear from the context.

Subgroups

A **subgroup** of a group is a subset of the elements of a group that is closed under the action of the original group. I.e. a set H is a subgroup of (G, \cdot) if

1. $h \in H \forall h \in H$
2. $h_1 \cdot h_2 \in H \forall h_1, h_2 \in H$

A subgroup is typically denoted $H < G$

A **normal subgroup** of a group is subgroup of a group which is closed under conjugation of the group. That is, N is a normal subgroup of G if it is a subgroup of G and

$$gng^{-1} \in H \forall n \in N, g \in G$$

Typically a normal subgroup is denoted $N \triangleleft G$

Direct product groups The *direct product* of two groups can be defined, for groups $(G, *)$, (H, \circ) , as

1. The underlying set is the Cartesian product $G \times H$, the ordered pairs $(g, h) \forall g \in G, h \in H$.

2. The binary operation is defined component-wise as

$$(g_1, h_1) \cdot (g_2, h_2) = (g_1 * g_2, h_1 \circ h_2)$$

The direct product is usually denoted with the \times operator. If $P = G \times H$, then the following is true:

1. The intersection $G \cap H$ is trivially the identity element of P
2. Every element of P can be expressed uniquely as the product of an element of G and an element of H .
3. All elements of G commute with elements of H .

In particular the final condition implies that both G and H are *both* normal subgroups of P .

Semidirect product groups A group G is a *semidirect product* of a subgroup $H \leq G$ and a normal subgroup $N \triangleleft G$ if one of the following equivalent condition holds:

- G is the product of the subgroups, $G = NH$, and the subgroups have the trivial intersection $N \cap H = e$.
- $\forall g \in G$, there is a unique $n \in N, h \in H$ such that $g = nh$
- $\forall g \in G$, there is a unique $n \in N, h \in H$ such that $g = hn$

Additional conditions are also sufficient, but not needed for this exposition. The semidirect product of two groups is denoted

$$G = N \rtimes H$$

The Euclidean group

Let $E(n)$ be the set of all isometries, i.e. all functions $T : \mathbb{R}^n \rightarrow \mathbb{R}^n$ such that

$$\|T(\mathbf{x}) - T(\mathbf{x}')\| = \|\mathbf{x} - \mathbf{x}'\|, \quad \text{for all } \mathbf{x}, \mathbf{x}' \in \mathbb{R}^n$$

We can identify $E(n)$ as a group if we define the group operation as the composition of two isometries by $T_1 \cdot T_2 := T_1 \circ T_2$ for all $T_1, T_2 \in E(n)$. Most importantly, we can identify all intuitive geometric transformations on \mathbb{R}^n as subgroups of $E(n)$:

1. **Translation:** For any vector $\mathbf{x} \in \mathbb{R}^n$, a translation by \mathbf{x} is given by the map $t_{\mathbf{x}} : \mathbb{R}^n \rightarrow \mathbb{R}^n, \mathbf{x}' \mapsto \mathbf{x} + \mathbf{x}'$. The set of all translations $T(n)$ forms a group.
2. **Rotoreflection:** The orthogonal group $O(n) = \{Q \in \mathbb{R}^{n \times n} | Q Q^T = I\}$ describes all reflections and subsequent rotations.
3. **Rotation:** The special orthogonal group $SO(n) = \{R \in O(n) | \det R = 1\}$ describes all rotations in \mathbb{R}^n .

A.2. Representations of Groups

Group representations are a powerful tool to describe the algebraic properties of geometric transformations:

Definition 2 (Group representation). *Let V be a vector space and $GL(V)$ be the **general linear group**, i.e. the group of all linear, invertible transformations on V with the composition $f \cdot g = f \circ g$ as group operation. Then a **representation** of a group G is a group homomorphism $\rho : G \rightarrow GL(V)$.*

For $V = \mathbb{R}^n$, this is the same as saying a group representation is a map $\rho : G \rightarrow \mathbb{R}^{n \times n}$ such that

$$\rho(g)\rho(h) = \rho(g \cdot h)$$

where the left hand side is typical matrix multiplication, and the right hand side is the group action. A representation of a group that is injective is commonly called a *faithful representation of a group*. Typical examples of faithful representations are:

1. For $SO(2)$, the rotation matrices given by

$$\rho(\theta) = \begin{bmatrix} \cos(\theta) & -\sin(\theta) \\ \sin(\theta) & \cos(\theta) \end{bmatrix}$$

and similarly for $SO(3)$.

2. For the permutation group, the permutation matrices. E.g for the group S_3 ,

$$\rho((13)(12)) = \begin{bmatrix} 0 & 1 & 0 \\ 0 & 0 & 1 \\ 1 & 0 & 0 \end{bmatrix}$$

One particularly useful result is that for *compact groups*, every representation is equivalent to a *unitary representation*, i.e. one such that $\forall g \in G$, $\rho(g)$ is a unitary operator. This therefore allows us when working with a representation of a compact group to always pick it to be unitary. This is useful as the identity $\rho(g)^T = \rho(g)^{-1}$ often makes calculations significantly easier.

Direct sums Given two representations, $\rho_1 : G \rightarrow GL(\mathbb{R}^n)$, $\rho_2 : G \rightarrow GL(\mathbb{R}^m)$, we can combine them together to give their *direct sum*, $\rho_1 \oplus \rho_2 : G \rightarrow GL(\mathbb{R}^{n+m})$, defined by

$$(\rho_1 \oplus \rho_2)(g) = \begin{bmatrix} \rho_1(g) & 0 \\ 0 & \rho_2(g) \end{bmatrix}$$

i.e the block diagonal matrix comprised of the individual representations. This sum generalises to summations of an arbitrary number of representations.

B. Proofs

B.1. Proof of proposition 1

Proposition 1. *Let P be a stochastic process over \mathcal{F}_ρ . Then the true posterior map $Z \mapsto P_Z$ is G -equivariant if and only if P is G -invariant, i.e. if and only if*

$$P = g.P \quad \text{for all } g \in G \quad (7)$$

Proof. Let us be given a distribution P over functions \mathcal{F}_d and $F \sim P$. Define $g.P$ to be the distribution of $g.F$. For any $\mathbf{x}_1, \dots, \mathbf{x}_n \in \mathbb{R}^2$ let $\rho_{\mathbf{x}_{1:n}}$ be the finite-dimensional marginal of P defined by

$$[F(\mathbf{x}_1), \dots, F(\mathbf{x}_n)]^T \sim \rho_{\mathbf{x}_{1:n}}$$

For simplicity, we assume here that $\rho_{\mathbf{x}_{1:n}}$ is absolutely continuous, i.e. has a density $\lambda_{\mathbf{x}_{1:n}}$.

Here, we assume that P is G -invariant, i.e. that the $g.F \sim g.P = P$. By Kolmogorov's theorem, this holds if and only if the finite-dimensional marginals agree, i.e. if and only if

$$\lambda_{\mathbf{x}_{1:n}}(\mathbf{y}_{1:n}) = \lambda_{g^{-1}\mathbf{x}_{1:n}}(\rho(h)^{-1}\mathbf{y}_{1:n}) \quad (19)$$

Comment: The left-hand side of this equation is the density of $[F(\mathbf{x}_1), \dots, F(\mathbf{x}_n)]^T$ evaluated at $[\mathbf{y}_1, \dots, \mathbf{y}_n]^T$ and the right-hand side is the density of $[g.F(\mathbf{x}_1), \dots, g.F(\mathbf{x}_n)]^T$ evaluated at $[\mathbf{y}_1, \dots, \mathbf{y}_n]^T$ (note that to do a change of variables after a transformation $\rho(h)$ one has to use the inverse $\rho(h)^{-1}$ in the density).

Given target points $\mathbf{x}'_{1:m}$, the conditional distribution of function values $\mathbf{y}'_{1:m}$ given $\mathbf{y}_{1:n}$ is given by the conditional density defined as

$$\begin{aligned} & \lambda_{\mathbf{x}'_{1:m}|\mathbf{x}_{1:n}}(\mathbf{y}'_{1:m}|\mathbf{y}_{1:n}) \\ &= \frac{\lambda_{\mathbf{x}_{1:n}, \mathbf{x}'_{1:m}}(\mathbf{y}_{1:n}, \mathbf{y}'_{1:m})}{\lambda_{\mathbf{x}_{1:n}}(\mathbf{y}_{1:n})} \end{aligned}$$

Let us be given now a context set $Z_C = \{(\mathbf{x}_i, \mathbf{y}_i)\}_{i=1}^n$ where here we assume $\mathbf{y}_i = f(\mathbf{x}_i)$. Our goal is to show that

$$P_{g.Z_C} = g.P_{Z_C}$$

i.e. the conditional distribution of F given $g.Z_C$ is the same as the conditional distribution of $g.F$ given Z_C . To prove this, we use that this is equivalent to

$$g^{-1}.P_{g.Z_C} = P_{Z_C}$$

and that by Kolmogorov's theorem (see [Øksendal \(2000\)](#)), this holds if and only if the finite dimensional marginals of both sides are equal. More exactly, given target points $\mathbf{x}'_1, \dots, \mathbf{x}'_m$, this holds if and only if the conditional of $g^{-1}F$ on the target points given $g.Z_C$ is the same as the conditional distribution of F on Z_C , i.e.

$$\lambda_{g, \mathbf{x}'_{1:m}|g, \mathbf{x}_{1:n}}(\rho(h)\mathbf{y}'_{1:m}|\rho(h)\mathbf{y}_{1:n}) = \lambda_{\mathbf{x}'_{1:m}|\mathbf{x}_{1:n}}(\mathbf{y}'_{1:m}|\mathbf{y}_{1:n})$$

Computing the left hand side:

$$\begin{aligned}
 & \lambda_{g, \mathbf{x}'_{1:m} | g, \mathbf{x}_{1:n}}(\rho(h)\mathbf{y}'_{1:m} | \rho(h)\mathbf{y}_{1:n}) \\
 &= \frac{\lambda_{g\mathbf{x}_{1:n}, g\mathbf{x}'_{1:m}}(\rho(h)\mathbf{y}_{1:n}, \rho(h)\mathbf{y}'_{1:m})}{\lambda_{g\mathbf{x}_{1:n}}(\rho(h)\mathbf{y}_{1:n})} \\
 &= \frac{\lambda_{\mathbf{x}_{1:n}, \mathbf{x}'_{1:m}}(\mathbf{y}_{1:n}, \mathbf{y}'_{1:m})}{\lambda_{\mathbf{x}_{1:n}}(\mathbf{y}_{1:n})} \\
 &= \lambda_{\mathbf{x}'_{1:m} | \mathbf{x}_{1:n}}(\mathbf{y}'_{1:m} | \mathbf{y}_{1:n})
 \end{aligned}$$

where the third line uses the assumption about the prior, replacing g^{-1} by g in By replacing g by g^{-1} in eq. (19), nominator and denominator agree and the theorem follows. Conversely, assuming that $Z \mapsto P_Z$ is equivariant, we can simply pick an empty context set $Z = \{\}$. In this case, $P_{g,Z} = P_Z = P$ and therefore equivariance implies $g.P = P$. \square

B.2. Proof of theorem 1

Theorem 1. *Let $G = T(n) \rtimes H$ and $\rho : H \rightarrow O(\mathbb{R}^d)$ be a fiber representation. A Gaussian process $\mathcal{GP}(\mathbf{m}, K)$ is G -equivariant for any noise parameter $\sigma^2 > 0$ if and only if it holds that*

1. $\mathbf{m}(\mathbf{x}) = \mathbf{m} \in \mathbb{R}^d$ is constant such that for all $h \in H$

$$\rho(h)\mathbf{m} = \mathbf{m} \quad (8)$$

2. K is fulfils the following two conditions:

- (a) K is **stationary**, i.e. for all $\mathbf{x}, \mathbf{x}' \in \mathbb{R}^n$

$$K(\mathbf{x}, \mathbf{x}') = K(\mathbf{x} - \mathbf{x}', \mathbf{0}) = \hat{K}(\mathbf{x} - \mathbf{x}') \quad (9)$$

- (b) K satisfies the **angular constraint**, i.e. for all $\mathbf{x}, \mathbf{x}' \in \mathbb{R}^n, h \in H$ it holds that

$$K(h\mathbf{x}, h\mathbf{x}') = \rho(h)K(\mathbf{x}, \mathbf{x}')\rho(h)^T \iff \quad (10)$$

$$\hat{K}(h\mathbf{x}) = \rho(h)\hat{K}(\mathbf{x})\rho(h)^T \quad (11)$$

If this is the case, we call K ρ -equivariant from now on.

Proof. By proposition 1, a GP model is G -equivariant if and only if the prior distribution $\mathcal{G}(\mathbf{m}, K)$ is G -invariant, i.e. if $F \sim P$, then also $g.F \sim P$. By Kolmogorov's theorem (see Øksendal (2000)), we can prove this only for finite-dimensional marginals, which are normal. Since a normal distribution is fully characterized by its pairwise covariances and means, invariance holds if and only if for all \mathbf{x}, \mathbf{x}' it holds that if $F \sim \mathcal{GP}(\mathbf{m}, K)$

$$\begin{aligned}
 \mathbf{m}(\mathbf{x}) &= \mathbb{E}(F(\mathbf{x})) \\
 &= \mathbb{E}(g.F(\mathbf{x})) \\
 &= \rho(h)\mathbf{m}(g^{-1}\mathbf{x}) \\
 &= g.\mathbf{m}(\mathbf{x})
 \end{aligned}$$

and

$$\begin{aligned}
 K(\mathbf{x}, \mathbf{x}') &= \text{Cov}(F(\mathbf{x}), F(\mathbf{x}')) \\
 &= \text{Cov}(g.F(\mathbf{x}), g.F(\mathbf{x}')) \\
 &= \text{Cov}(\rho(h)F(g^{-1}\mathbf{x}), \rho(h)F(g^{-1}\mathbf{x}')) \\
 &= \rho(h)\text{Cov}(F(g^{-1}\mathbf{x}), F(g^{-1}\mathbf{x}'))\rho(h)^T \\
 &= \rho(h)K(g^{-1}\mathbf{x}, g^{-1}\mathbf{x}')\rho(h)^T
 \end{aligned}$$

Let us assume that this equation holds. Then picking $g = t_{\mathbf{x}'}$ implies that

$$\begin{aligned}
 \mathbf{m}(\mathbf{x}) &= \mathbf{m}(\mathbf{x} - \mathbf{x}') \\
 K(\mathbf{x}, \mathbf{x}') &= K(\mathbf{x} - \mathbf{x}', 0)
 \end{aligned}$$

i.e. \mathbf{m} is constant and K is stationary. Similiarly, picking $g = h$ implies eq. (8) and eq. (10).

To prove the opposite direction, we can go these computations backwards if we assume that the conditions from the theorem are satisfied. \square

B.3. Proof of proposition 2

Proposition 2. *A conditional process model is G -equivariant if and only if the mean and covariance feature maps are G -equivariant, i.e. if it holds*

$$\mathbf{m}_{g,Z} = g.\mathbf{m}_Z \quad (14)$$

$$\Sigma_{g,Z} = g.\Sigma_Z \quad (15)$$

for all $g \in G$ and context sets Z .

Proof. Let Q_{Z_C} be the output of the model serving as the approximation of posterior distribution P_{Z_C} . It holds Q_{Z_C} is G -equivariant if and only if $Q_{g,Z_C} = g.Q_{Z_C}$. If $F \sim Q_{Z_C}$, it holds by standard facts about the normal distribution

$$\begin{aligned}
 g.F(\mathbf{x}) &= \rho(h)F(g^{-1}\mathbf{x}) \\
 &\sim \mathcal{N}(\rho(h)\mathbf{m}_{Z_C}(g^{-1}\mathbf{x}), \rho(h)\Sigma_{Z_C}(g^{-1}\mathbf{x})\rho(h)^T) \\
 &= \mathcal{N}(g.\mathbf{m}_{Z_C}(\mathbf{x}), g.\Sigma_{Z_C}(\mathbf{x}))
 \end{aligned}$$

which gives the one-dimensional marginals of $g.Q_{Z_C}$. By the conditional independence assumption, $g.Q_{Z_C} = Q_{g,Z_C}$ if and only if their one-dimensional marginals agree, i.e. if for all \mathbf{x}

$$\mathcal{N}(\mathbf{m}_{g,Z_C}(\mathbf{x}), \Sigma_{g,Z_C}(\mathbf{x})) = \mathcal{N}(g.\mathbf{m}_{Z_C}(\mathbf{x}), g.\Sigma_{Z_C}(\mathbf{x}))$$

This is equivalent to $\mathbf{m}_{g,Z_C} = g.\mathbf{m}_{Z_C}$ and $\Sigma_{g,Z_C} = g.\Sigma_{Z_C}$, which finishes the proof. \square

B.4. Proof of theorem 2

Theorem 2 (EquivDeepSets). *A function $\Phi : \mathcal{Z}_{\rho_{in}}^1 \rightarrow \mathcal{F}_{\rho_{out}}$ is G -equivariant and permutation invariant if and only if it*

has a representation of the form

$$\Phi(Z) = \Psi(E(Z))$$

for all $Z = \{(\mathbf{x}_i, \mathbf{y}_i)\}_{i=1}^m \in \mathcal{Z}_{\rho_{in}}^1$ where

1. $E(Z) = \sum_{i=1}^m K(\cdot, \mathbf{x}_i) \phi(\mathbf{y}_i)$
2. $\phi(\mathbf{y}) = (1, \mathbf{y})^T \in \mathbb{R}^{d+1}$.
3. $K : \mathbb{R}^n \times \mathbb{R}^n \rightarrow \mathbb{R}^{(d+1) \times (d+1)}$ is an ρ_E -equivariant strictly positive definite kernel (see theorem 1).
4. $\Psi : \mathcal{F}_{\rho_E} \rightarrow \mathcal{F}_{\rho_{out}}$ is a G -equivariant functions.

where we coin $\rho_E = \mathbf{1} \oplus \rho_{in}$ the embedding representation.

Additionally, by imposing extra constraints (see appendix B.4), we can also ensure that Φ is continuous.

Proof. **Step 1: Injectivity of E .**

We first want to show that under the given conditions E is injective. Let $\mathcal{H} \subset \{f : \mathbb{R}^n \rightarrow \mathbb{R}^{d+1}\}$ be the RKHS of K (see Álvarez et al. (2012)).

So let us assume that for two data sets $Z = \{(\mathbf{x}_i, \mathbf{y}_i)\}_{i=1}^m$ and $Z' = \{(\mathbf{x}'_j, \mathbf{y}'_j)\}_{j=1}^n$ we have that $E(Z) = E(Z')$. This is equivalent to:

$$\sum_{i=1}^m K(\cdot, \mathbf{x}_i) \begin{pmatrix} 1 \\ \mathbf{y}_i \end{pmatrix} = \sum_{j=1}^n K(\cdot, \mathbf{x}'_j) \begin{pmatrix} 1 \\ \mathbf{y}'_j \end{pmatrix}$$

Let f be in the RKHS of K , then by using the reproducing property of the RKHS of K , we get

$$\sum_{i=1}^m f(\mathbf{x}_i)^T \begin{pmatrix} 1 \\ \mathbf{y}_i \end{pmatrix} = \sum_{j=1}^n f(\mathbf{x}'_j)^T \begin{pmatrix} 1 \\ \mathbf{y}'_j \end{pmatrix}$$

Let us choose an arbitrary \mathbf{x}_k . By the assumption that K is strictly positive definite, we can pick f such that $f(\mathbf{x}_k) = (1, 0, \dots, 0)^T$, $f(\mathbf{x}_i) = 0$ for all $i \neq k$ and $f(\mathbf{x}'_j) = 0$ for all $\mathbf{x}_j \neq \mathbf{x}_k$. We then get

$$1 = \sum_{j=1}^n 1_{\mathbf{x}'_j = \mathbf{x}_k}$$

Therefore, there is exactly one j such that $\mathbf{x}'_j = \mathbf{x}_k$. Turning the argument around, we get that $n = m$ and that $(\mathbf{x}_1, \dots, \mathbf{x}_n)$ is a permutation of $(\mathbf{x}'_1, \dots, \mathbf{x}'_n)$. Therefore, we can now assume that $\mathbf{x}_i = \mathbf{x}'_i$ for all $i = 1, \dots, n$.

Pick now f such that $f(\mathbf{x}_i) = (0, \mathbf{y})^T$ for some $\mathbf{y} \in \mathbb{R}^d$. Then it follows that

$$\mathbf{y}^T \mathbf{y}_i = \mathbf{y}^T \mathbf{y}'_i$$

Since this holds for all \mathbf{y} , we can conclude that $\mathbf{y}_i = \mathbf{y}'_i$. In sum, this shows

Step 2: Equivariance of E .

Let $Z = \{(\mathbf{x}_1, \mathbf{y}_1), \dots, (\mathbf{x}_m, \mathbf{y}_m)\}$ be a context set and $g = t_{\mathbf{x}} h \in G$. Then it follows that

$$\begin{aligned} E_{g, Z} &= \sum_{i=1}^m K(\cdot, g\mathbf{x}_i) \begin{pmatrix} 1 \\ \rho_{in}(h)\mathbf{y}_i \end{pmatrix} \\ &= \sum_{i=1}^m K(\cdot, g\mathbf{x}_i) \rho_E(h) \begin{pmatrix} 1 \\ \mathbf{y}_i \end{pmatrix} \\ &= \sum_{i=1}^m \rho_E(h) K(g^{-1}\cdot, \mathbf{x}_i) \rho_E(h)^T \rho_E(h) \begin{pmatrix} 1 \\ \mathbf{y}_i \end{pmatrix} \\ &= \rho_E(h) E_Z(g^{-1}\cdot) \\ &= g \cdot E_Z \end{aligned}$$

Step 3: Universality and equivariance of the representation.

Assuming that Ψ is G -equivariant, it follows that Φ is G -equivariant since it is a composition of equivariant maps Ψ and E .

Conversely, if we assume that Φ is an equivariant function. We can define $\Psi = \Phi \circ E^{-1}$ on the image of E (and constant zero outside of the image). Since E is equivariant, also E^{-1} is and therefore Ψ is equivariant as a composition of equivariant maps.

This finishes the proof of the main statement of the theorem.

Additional step: Continuity of Φ . We can enforce continuity of Φ by assuming:

1. We restrict Φ on a subset $\mathcal{Z}' \subset \mathcal{Z}_{\rho}^1$ which is topologically closed, closed under permutations and closed under actions of G .
2. K is continuous and $K(\mathbf{x}, \mathbf{x}') \rightarrow 0$ for $\|\mathbf{x} - \mathbf{x}'\| \rightarrow 0$.
3. Ψ is continuous.

The proof of this follows directly from the proof of the ConvDeepSets theorem from Gordon et al. (2019), along with the additional conditions proved above. \square

One particular difference from the ConvDeepSets theorem is that we only prove this for multiplicity 1 sets, whereas ConvDeepSets is proved for arbitrary multiplicity. This is due to the fact that the authors do not know of an analogue to the sum-of-powers mapping ϕ used in the construction for the scalar case for vector data that also obeys H -equivariance.

C. Equivariant Kernels for GPs

A divergence free kernel is a matrix valued kernel $\Phi : \mathbb{R}^n \rightarrow \mathbb{R}^{n \times n}$ such that its columns are divergence free. That is

$\nabla^T(\Phi(\mathbf{x})c) = 0 \forall c \in \mathbb{R}^n$. This ensures that and field given by $f(\mathbf{x}) = \sum_{i=1}^N \Phi(\mathbf{x}, \mathbf{x}_i)c_i \forall c_i, \mathbf{x}_i \in \mathbb{R}^n$ is divergence free. The kernels used in this work were introduced by [Macêdo & Castro \(2010\)](#). In particular we use the curl and divergence free kernels defined as, for all $\mathbf{x}, \mathbf{x}' \in \mathbb{R}^2$:

$$K_0(\mathbf{x}, \mathbf{x}') = \frac{1}{l^2} \exp\left(-\frac{\|\mathbf{x} - \mathbf{x}'\|^2}{2l^2}\right)$$

$$A_{\mathbf{x}, \mathbf{x}'} = \mathbf{I} - \frac{(\mathbf{x} - \mathbf{x}')(\mathbf{x} - \mathbf{x}')^T}{l^2}$$

$$B_{\mathbf{x}, \mathbf{x}'} = \frac{(\mathbf{x} - \mathbf{x}')(\mathbf{x} - \mathbf{x}')^T}{l^2} + \left(1 - \frac{\|\mathbf{x} - \mathbf{x}'\|^2}{l^2}\right) \mathbf{I}$$

$K_{\text{curl}} = K_0(\mathbf{x}, \mathbf{x}')A_{\mathbf{x}, \mathbf{x}'}$, $K_{\text{div}}(\mathbf{x}, \mathbf{x}') = K_0(\mathbf{x}, \mathbf{x}')B_{\mathbf{x}, \mathbf{x}'}$ are curl free and divergence free respectively.

D. Experimental details

For the implementation, we used *PyTorch* ([Paszke et al., 2017](#)) as a library for automatic differentiation and for computation we used a Graphics processing unit (GeForce GTX 1080).

To set up the EquivCNP model, we stacked equivariant convolutional layers with NormReLU activation functions in between as a decoder. The smoothing step was performed with a scalar RBF-kernel where the length scale was included in the computation graph and optimized during training. All hidden layers of the decoder use the regular representation ρ_{reg} as a fiber representation ρ of the hidden layers of the decoder if the fiber group H is C_N or D_N and the identity representation ρ_{Id} for infinite fiber groups. This choice gave the best results and is also consistent with observations in supervised learning problems ([Weiler & Cesa, 2019](#)). For the encoder E , we found that the choice of kernels K does not lead to significant differences in performance. Therefore, the results stated here used a diagonal RBF-kernel where we let the length-scale variable as a hyperparameter. Similar to [Gordon et al. \(2019\)](#), we found that the additional step in the encoder of normalizing all channels except the density channel by the density channel, improved performance. This operation is clearly invertible and preserves equivariance.

D.1. GP experiments

Details for GP data sets. For every sample we have chosen a randomly orientated grid $\mathcal{G} \subset [-10, 10]^2$ spread in a circle around the origin and sampled a Gaussian process on it with kernel K with $l = 5$. To a set of pairs $\{(\mathbf{x}, F(\mathbf{x}))\}_{\mathbf{x} \in \mathcal{G}}$, we add random noise $\epsilon \sim \mathcal{N}(0, \sigma^2)$ with $\sigma = 0.05$ on $F(\mathbf{x})$. During training, we randomly split a data set in a context set and in target set. The maximum size of a context set is set to 50. As usually done for CNPs ([Garnelo et al., 2018a](#)), the target set includes the context set during training.

D.2. ERA5 wind data

The ERA5 data set consists of weather parameters on a longitude-latitude grid around the globe. We extracted the data for all points surrounding Memphis, Tennessee, with a distance of less than 520km giving us approximately 1200 grid points per weather map.

The weather variables we use are temperature, pressure and wind and we picked hourly data from the winter months December, January and February from years 1980 to 2018. Every sample corresponds to one weather map of temperature, pressure and wind in the region at one single point in time. Finally, we splitted the data set in a training set of 35000, a validation set of 17500 and test set of 17500 weather maps. Similarly, we proceeded for the data set from Southern China.